Journal of Materials Chemistry C

Accepted Manuscript

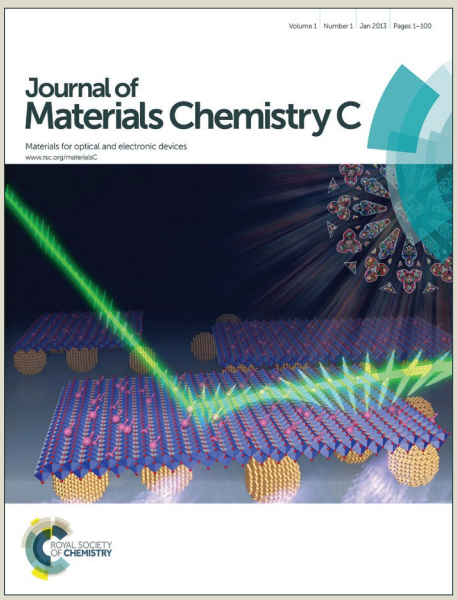

ROYAL SOCIETY OF CHEMISTRY

www.rsc.org/materialsC

Journal Name

RSCPublishing

ARTICLE

Metal Nanowire Percolation Micro-Grids Embedded in Elastomer for Stretchable and Transparent Conductors†

Sang-Min Park,[a] Nam-Su Jang,[b] Sung-Hun Ha,[b] Kang Hyun Kim,[b] Dong-Wook Jeong,[b] Jeonghyo Kim,[c] Jaebeom Lee,[c] Soo Hyung Kim[a,b] and Jong-Man Kim*[a,b]

Cite this: DOI: 10.1039/x0xx00000x

Received ooth January 2012,
Accepted ooth January 2012

DOI: 10.1039/x0xx00000x

www.rsc.org/

Next-generation stretchable optoelectronics require functional electric conductors with mechanical stretchability and optical transparency. We present a new class of highly stretchable and transparent conductors based on silver nanowire (AgNW) percolation micro-grids embedded in an elastomeric substrate. These are prepared by simple spray-coating and subsequent adhesive-tape-assisted contact-removal of the AgNWs. The synergetic combination of the percolated NWs and regular micro-grid geometry in an integrated form makes it possible to achieve uniform, reproducible, and predictable performance of the resulting AgNW micro-grids and ensure good stretchability. The fabricated device shows superior optoelectronic performance with a sheet resistance of 26.1 Ω/sq and an optical transmittance of 85.8 %. In addition, the device can reversibly accommodate various mechanical deformations, such as stretching, bending, and twisting.

Introduction

Over the past few decades, transparent conductors (TCs) have attracted much attention, since they are essential components in numerous optoelectronic devices, including displays, photovoltaics, touch panel screens, light-emitting diodes (LEDs), and smart windows.[1] With increasing interest in next-generation electronics such as foldable optoelectronics and skin-mountable human interfaces, considerable efforts have recently been devoted to developing TCs with mechanical flexibility and stretchability. Indium tin oxide (ITO) has been regarded as the best choice for TCs in many applications, due to its excellent optoelectronic properties (low sheet resistance and high optical transmittance).[2-4] However, the brittleness of ITO critically limits its practical use in emerging flexible and stretchable electronics.[5,6]

Many alternative materials and fabrication techniques have been extensively studied to overcome the limitations of ITO for the development of high-performance stretchable TCs. Functional conductive nanomaterials such as metal nanowires (mNWs)[7-13] and carbon nanotubes (CNTs)[14,15] can be employed as conductive pathways for charge transport after being assembled into a network on elastomeric substrates. The interconnected mNW networks can facilitate appreciable retention of the electrical conductivity upon bending or even stretching while providing optical transparency through the spaces between NWs. In addition, the solution-processability enabled by various wet-coating methods results in simple and low-cost fabrication of stretchable TCs. Nevertheless, this approach is unsuitable for reproducibly achieving uniform performance over large areas mainly due to the random geometries that can cause large variations in the distribution of the nanomaterials.

Conductive CNT sheets can be integrated with elastomeric substrates to form stretchable TCs.[16-22] Although they could potentially yield superior stretchability due to the unique architectures, the electrical and optical performance may not meet the requirements for some optoelectronic applications. Some conductive and transparent films such as graphene[23] and poly(3,4-ethylenedioxythiophene):poly(styrenesulfonic) (PEDOT:PSS)[24] have been demonstrated as stretchable TCs by transferring them onto pre-strained elastomeric substrates and then releasing them. The optoelectronic properties can be controlled through the number of film layers. However, the stretchability of the TCs may be significantly restricted because it strongly depends on the pre-strain level of the elastomeric substrate. Moreover, it would be very difficult to obtain low sheet resistance without sacrificing the optical transparency. Compared to conductive thin-films, mesh architectures with a

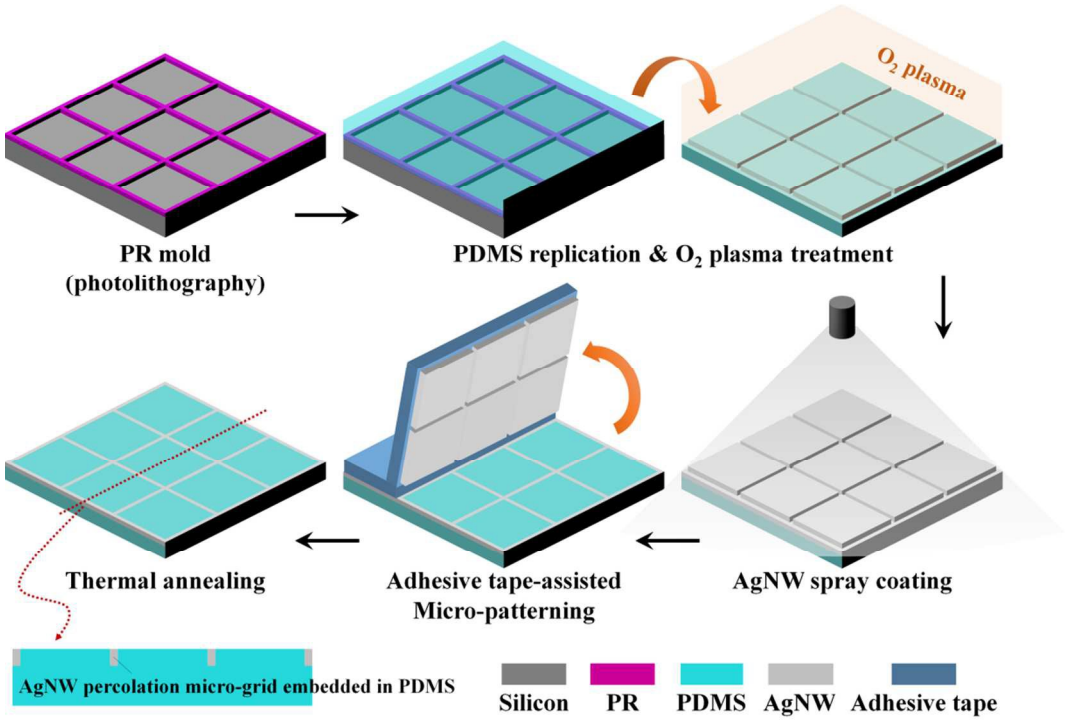

Fig. 1 Schematic illustration of fabrication sequences for the proposed stretchable AgNW percolation micro-grids.

fully interconnected network made of highly conductive metals such as platinum[25] and gold[26] are potential candidates for enhancing stretchability while achieving good optoelectronic performance. The electrical and optical properties of the TCs can also be optimized by precisely controlling the fabrication conditions that determine the height and thickness of mesh structures, and the opening area. However, the fabrication is expensive and complex, since it involves high-vacuum processes (metal sputtering and evaporation) and cumbersome wet transfer of the metal meshes, which hinder low-cost and large-area fabrication. Furthermore, the changes in electrical properties may be irreversible when subjected to a certain critical strain due to possible plastic deformation of the continuously interconnected metal mesh.

Here we report silver nanowire (AgNW) percolation micro-grid structures for high-performance stretchable TCs. Highly percolated AgNW networks were selectively embedded in grid-shaped polydimethylsiloxane (PDMS) micro-trenches by a simple combination of spray-coating and subsequent adhesive-tape-assisted contact-removal processes. The fabrication method makes it possible to simply and precisely prepare arbitrary shapes of NW percolation micro-patterns guided by pre-defined PDMS micro-trenches. In addition, the solution-processability can facilitate low-cost and large-area fabrication. The integration of mNW networks with micro-grid structures also demonstrates several advantages over other technologies. The AgNW micro-grids allow to achieve uniform, reproducible, and predictable optoelectronic performance due to their regular geometry. In addition, the NW percolation network structures can withstand high strains above the fracture limit without permanent electrical or structural failure, resulting in both considerable stretchability and reversibility.

Experimental

Synthesis of AgNWs

AgNWs were synthesized based on a $CuCl_2$-mediated polyol process.[27] 10 mL of ethylene glycol (EG; Daejung Chemical & Metal) was kept in an oil bath for 1 hr while heating at 160 °C and magnetically stirring at 360 rpm. 40 μL of copper (II) chloride ($CuCl_2$; 4 mM; Samchun Chemical) was then added to the heated EG. After maintaining for 15 min, 3 mL of 0.094 M silver nitrate ($AgNO_3$; Sigma-Aldrich) solution in EG and 3 mL of 0.147 M polyvinyl pyrrolidone (PVP; Alfa Aesar) solution in EG were injected to the heated EG at a rate of 0.3 mL/min using a two-channel syringe pump (Legato 111, KD Scientific) while continuously heating and stirring for 1 hr. The synthesized AgNWs were purified in 50 mL of acetone and 50 mL of ethanol by centrifuging three times each at 2000 rpm for 20 min using a commercial centrifuge (TD4Z-WS, Nasco Korea). The synthesized AgNWs had an average length of ~40 μm and average diameter of ~195 nm (see Fig. S1†). These were dispersed in ethanol for spray-coating.

Fabrication of AgNW Percolation Micro-Grids

A PDMS substrate with micro-trenches was first prepared by replicating from a polymeric mold using a soft-lithographic technique. A ~20-μm-thick photoresist (PR; THB-151N, JSR

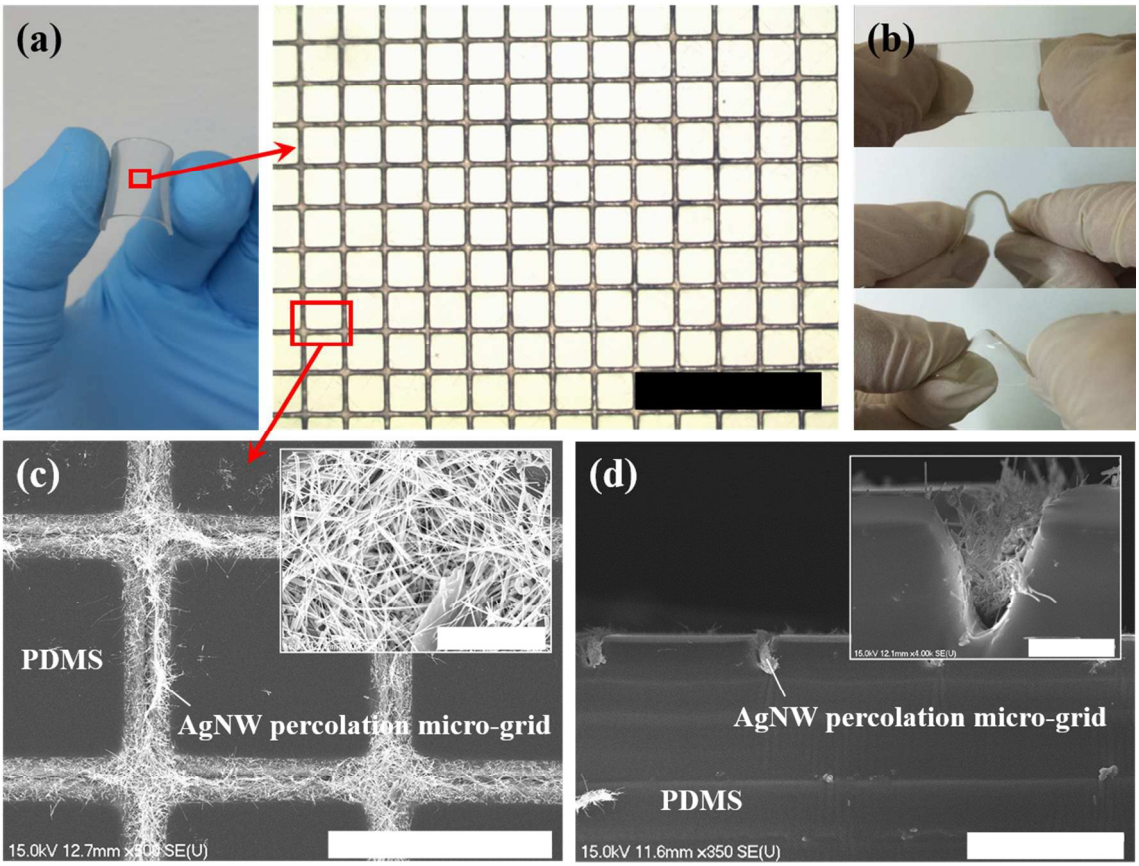

Fig. 2 Fabrication results of the stretchable AgNW micro-grid. (a) digital and magnified microscope images of the fabricated stretchable AgNW micro-grid (scale bar: 500 μm), (b) digital images of the fabricated device under various mechanical deformations, (c) top-view SEM image of the device; scale bar: 100 μm (inset: enlarged SEM image of AgNW percolation network in the PDMS micro-trench; scale bar: 10 μm), and (d) cross-sectional SEM image of the device; scale bar: 100 μm (inset: enlarged SEM image of AgNW percolation network embedded in the PDMS micro-trench; scale bar: 10 μm).

Micro) mold with a grid width of 10 μm was formed on a silicon substrate. A PDMS prepolymer (Sylgard 184, Dow Corning) mixed with a curing agent at a weight ratio of 10:1 was then poured onto the mold substrate and subsequently degassed in a vacuum desiccator for 1 hr to remove all air bubbles. After thermally curing in a convection oven at 70 °C for 1 hr, the ~1-mm-thick PDMS substrate was carefully peeled off from the mold substrate.

50 mL of the AgNW solution with a concentration of 20 mg/mL was then sprayed onto the micro-grid electrode region (1.5 cm × 1.5 cm) of the PDMS substrate using a commercial airbrush (DH-115, Sparmax) with a nozzle diameter of 0.35 mm. Prior to the coating process, the PDMS substrate was exposed briefly to O_2 plasma to enhance its wetting by making the surface hydrophilic. The coating process was conducted on a hotplate at 120 °C to promote rapid evaporation of the solvent. During coating, the nozzle-to-substrate distance and airbrush pressure were constantly maintained at ~15 cm and 0.5 MPa, respectively. The AgNW percolation micro-grids were then defined in the micro-trenches by selectively removing AgNWs deposited on the top surface of the PDMS substrate using an adhesive tape wrapped on a hand roller. Finally, the sample was thermally annealed at 200 °C for 20 min to fuse the NW junctions and reduce their contact resistance.

Characterization

The morphology of the AgNWs and AgNW micro-grids was investigated using an optical microscope (BX60M, Olympus) and a field emission scanning electron microscope (FESEM; S4700, Hitachi). The sheet resistance (R_s) was calculated according to the relationship $R_s = R \times (w/l)$, where w and l are the width and length of the TC region in the sample, respectively, and R is the electrical resistance obtained from two-probe measurements.[28,29] The electrical resistance was measured using a digital multimeter (U1253B, Agilent Technologies) capable of measuring up to 500 MΩ with a resolution of 0.01 MΩ. For the measurement, the probing electrodes at each end of the sample were electrically wired with a silver paste. The sheet resistance was taken from more than three samples and averaged for each model with different grid-to-grid pitch. Optical transmittance spectra were recorded

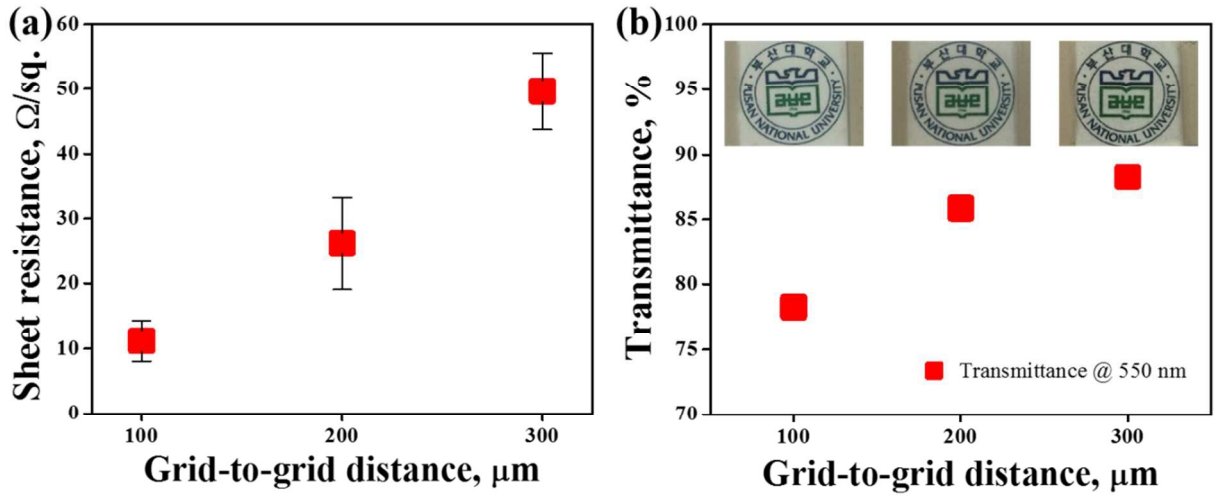

Fig. 3 Optoelectronic performance of the fabricated stretchable AgNW micro-grids as a function of grid-to-grid distance (100, 200, and 300 μm) with a fixed grid width of 10 μm. (a) sheet resistances, and (b) optical transmittances at 550-nm wavelength (inset: digital images of each device placed on a logo of our institution).

by a UV-visible spectrophotometer (Evolution 20, Thermo Scientific) at a wavelength range of 400 nm to 800 nm.

All the mechanical tests were performed after forming a thin PDMS coating layer on the AgNW micro-grids. For the stretching test, tensile strain was applied to the sample using a commercial motorized stage (JSV-H100, JISC) equipped with a push-pull force gauge (HF-10, JISC). The test was conducted at a stretching and releasing speed of 1 mm/min, and the corresponding electrical resistance was recorded in real time using a computer interfaced with a digital multimeter through a data cable (RS-232). Bending and twisting tests were performed by measuring the resistance at various bending radii and twisting angles, respectively.

The electrical robustness of the stretchable AgNW micro-grids was investigated under various mechanical deformations, such as stretching, bending, and twisting. A simple LED circuit was constructed by connecting the fabricated device to a LED and a power supply (E3649A, Agilent Technologies) in series. The power supply was used to apply the turn-on voltage (3 V) of the LED, and images of the circuit in each deformed state were taken with a digital camera.

Results and discussion

The proposed stretchable AgNW micro-grids were fabricated by filling AgNWs into grid-shaped PDMS micro-trenches using spray-coating and subsequent contact-removal process (hereafter, coating-and-removal (C/R) process for convenience), as shown in Fig. 1. Prior to fabrication, the effectiveness of the adhesive-tape-assisted contact-removal process was examined by comparing the optical transmittance (T) of flat PDMS substrate (thickness: ~1 mm) in three different states: initial (bare), AgNW-coated, and contact-removed, as shown in Fig. S2†. Although the bare PDMS substrate (T = 92.5 % at 550 nm) became quite hazy after spray-coating AgNWs (T = 50.1 %), the transmittance was almost recovered to that of the bare PDMS by removing most of the deposited AgNWs through the contact-removal process (T = 90.8 %). This simple process can be easily integrated with the PDMS micro-trenches to embed the AgNW percolation networks into them.

Fig. 2a shows digital and magnified microscope images of the fabricated stretchable AgNW micro-grid with quite uniform micro-grid structures over a large area. The digital images in Fig. 2b also demonstrate that the device is highly stretchable, bendable, and twistable. The top-view SEM images in Fig. 2c show that the highly percolated AgNW networks were well defined in a micro-grid form, revealing transparent window areas between the grid lines.

It is quite difficult to conformally fill the ~40-μm-long AgNWs into the 10-μm-wide trenches, but multiple C/R cycles can facilitate this, as shown in the cross-sectional SEM images in Fig. 2d. The sheet resistance was gradually decreased with increasing the C/R cycle number and eventually reached 13.3 Ω/sq after five cycles (10 mL of AgNW solution per a cycle; see Fig. S3a†). In the case of a single C/R process with 50 mL of AgNW solution, the sheet resistance was measured as 215.6 Ω/sq, which means that AgNWs covering the trenches critically hindered further penetration of AgNWs (Fig. S3b and c†). This clearly suggests that multiple C/R processes are greatly helpful for achieving high electrical performance of the stretchable AgNW micro-grids by making it possible to conformally fill the AgNWs into the micro-trenches. In most mNW-based TCs, the optoelectronic performance strongly depends on the uniformity of percolated mNW networks. However, a difficulty in controllable manipulation of NWs is still one of the critical hindrances to reproducible fabrication. In this regard, the C/R process is highly favorable for the reliable fabrication of stretchable TCs because the optoelectronic properties of the

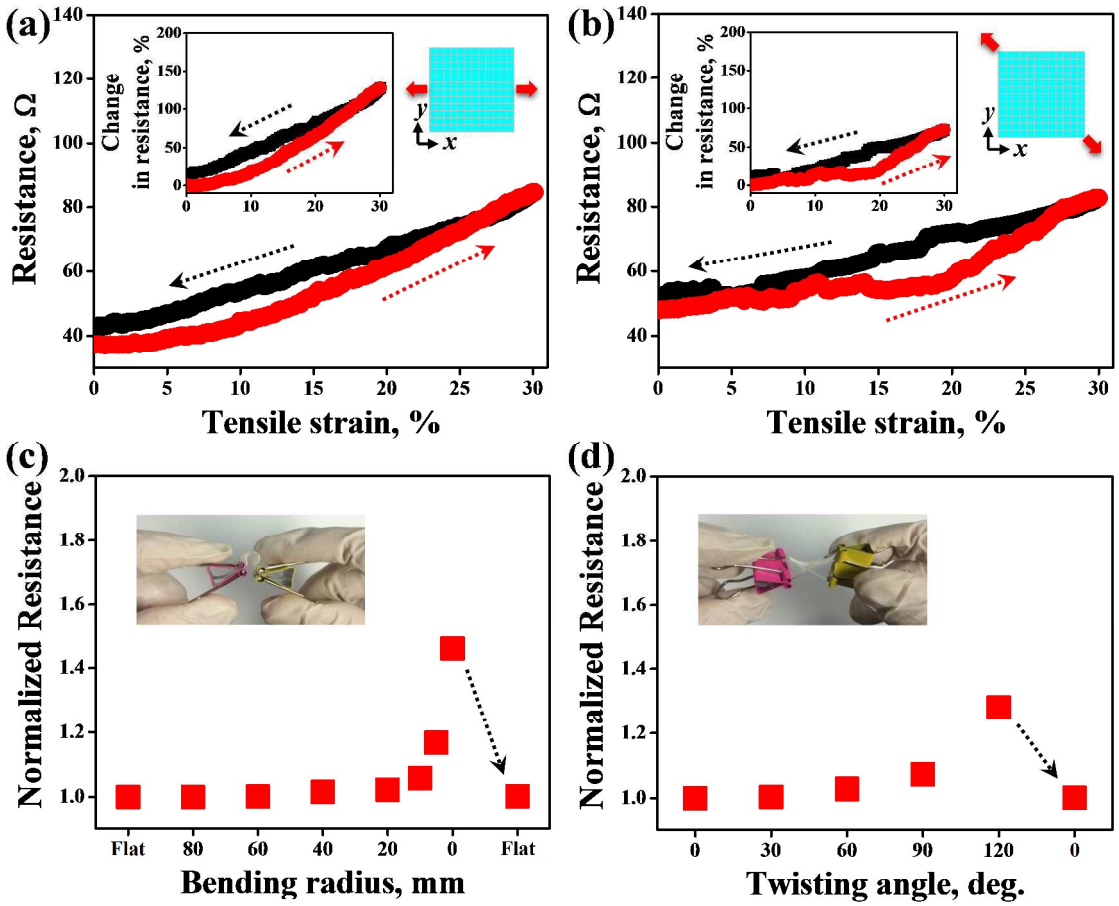

Fig. 4 Electrical performance of the fabricated stretchable AgNW micro-grid under various mechanical deformations. Electrical resistances of the device in response to tensile strain of up to 30 % applied along (a) the x-direction and (b) 45 ° (inset: resistance changes in a percentage form). Normalized resistance of the device (d) under bending up to a minimum bending radius of < 1 mm and (e) under twisting up to 120 ° (inset: digital images of the devices under bending and twisting deformations).

resulting devices are relatively insensitive to the uniformity in AgNW coating.

In general, the optoelectronic characteristics of micro-grids can be optimized by controlling a filling factor (FF) that is represented by the portion covered by conductive grid pattern with respect to whole area (i.e., FF = $w_g/(d_{g\text{-}g}+w_g)$ where w_g is a grid width and $d_{g\text{-}g}$ is a grid-to-grid distance.). In this regard, both the sheet resistance and optical transmittance of the stretchable AgNW micro-grids could be easily controlled by varying $d_{g\text{-}g}$ with a fixed w_g. Fig. 3a shows the sheet resistances of the fabricated devices as a function of $d_{g\text{-}g}$ (100, 200, and 300 μm) with w_g of 10 μm. The sheet resistance was linearly proportional to $d_{g\text{-}g}$. Moreover, reasonable deviations were achieved for each model although the surface morphologies might be varied due to the manual process. This suggests that the multiple C/R process is quite reproducible and the performance uniformity can be further enhanced by automating the fabrication process. A considerably low sheet resistance of 11.2 Ω/sq (average) was achieved when $d_{g\text{-}g}$ = 100 μm, which originates both from the high FF and the highly interconnected geometry of AgNWs in the PDMS micro-trenches. To verify the electrical robustness of the fabricated device under repetitive mechanical deformations, cyclic stretching/releasing test was conducted for up to 30 cycles with a maximum strain of 30 %. The normalized electrical resistances in the released state of each cycle were similarly maintained without appreciable deviations, as shown in Fig. S4†. This demonstrates that reversible sliding in the percolated network of AgNWs is quite stable even under repetitive stretch and release.

Fig. 3b shows the optical transmittance at a wavelength of 550 nm for different $d_{g\text{-}g}$ with digital images of three representative devices placed on a logo of our institution. Full transmittance spectra obtained at wavelength ranging from 400 nm to 800 nm for each device are provided in Fig. S5†. The transmittance was gradually increased with increasing $d_{g\text{-}g}$, exceeding 80 % for $d_{g\text{-}g}$ of ≥ 200 μm. This is due to the fact that the scattering of incident light on the grid pattern is accordingly reduced with decreasing the FF. In particular, the device with $d_{g\text{-}g}$ = 200 μm produced a low sheet resistance of 26.1 Ω/sq

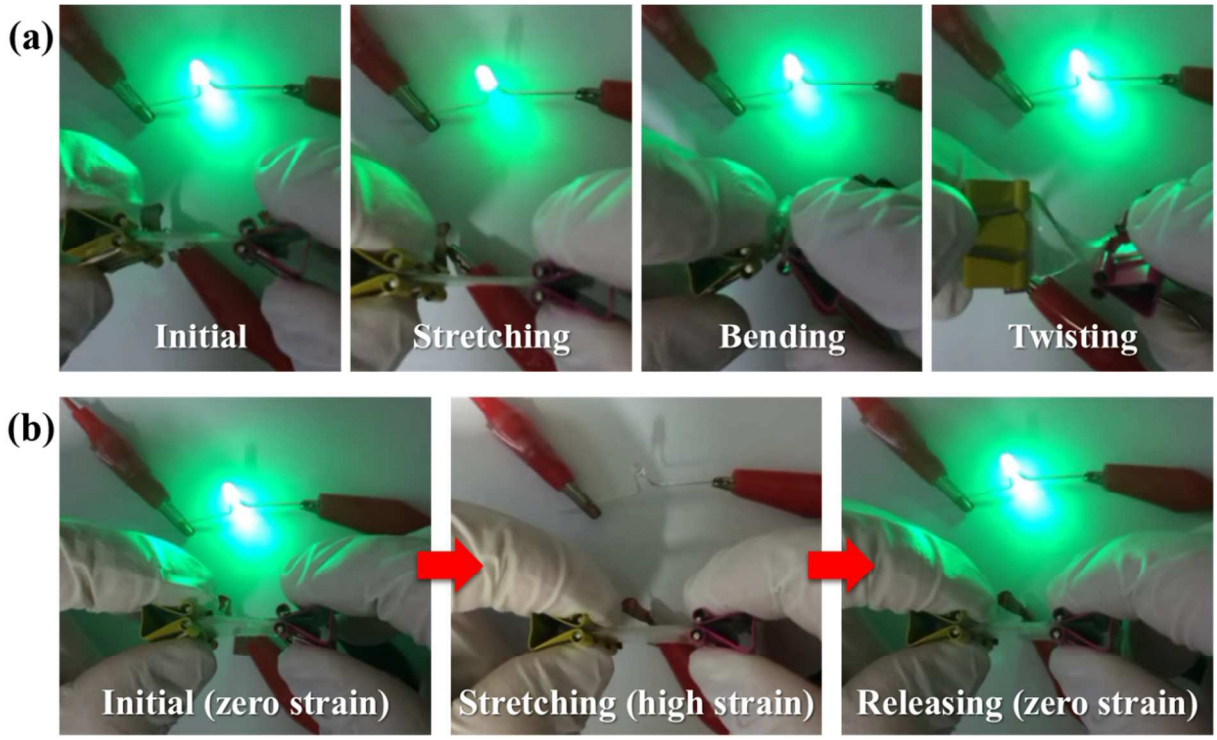

Fig. 5 Digital images of LED circuits integrated with the stretchable AgNW micro-grid (a) under various mechanical deformations (stretching, bending and twisting) and (b) upon stretching to ~36 % and releasing to 0 %.

(average) and high transmittance of 85.8 % (at 550 nm), which are comparable to the values for commercial ITO.[30]

To evaluate the performance of the AgNW micro-grids as stretchable electrodes, we investigated their electrical properties under various mechanical deformations. Fig. 4a shows the change in electrical resistance of the stretchable AgNW micro-grid in response to an applied tensile strain of up to 30 % in the *x*-direction. When stretched to 30 %, the resistance increased by ~47 Ω (~127 %) compared to the initial value (37.2 Ω), which is favorable for various next-generation stretchable electronics. Importantly, the resistance almost returned to its starting value when the applied strain was fully released, indicating an increase of only ~5.6 Ω (~15 %) compared to the initial state. The electrical properties of the stretchable AgNW micro-grid were also quite reversible, even when subjected to higher tensile strains of up to 50 % (Fig. S5†). The desirable recoverability can be attributed to reversible sliding of the AgNWs adjacent to each other in the percolated network upon stretching and releasing.[31] During stretching, AgNWs that are touching each other in the initial state may slide in each strained direction, which results in maintaining the electrical contact for current flow. Although some inter-NW junctions can be lost when imposing tensile strains beyond the specific facture limit, most of them would return to the original geometry upon releasing, as shown in Fig. S6†.

By virtue of the square geometry, the device was also highly stretchable (~35 Ω (~73 %) increase at 30 % strain) and reversible (~4 Ω (~8 %) increase compared to the initial state) in the strain direction of 45°, as shown in Fig. 4b. In particular, the increase in the resistance was smaller than the case of stretching in the *x*-direction probably due to the formation of the rhombic structure upon stretching. This suggests that the stretchable AgNW micro-grids can retain their electrical performance upon strain in any direction. The stretchable AgNW micro-grids were also found to be electrically robust under bending and twisting deformations. Fig. 4c shows the normalized resistance (R_{norm}) as a function of bending radius. The largest increase in the electrical resistance (R_{norm} = 1.46) was observed at a bending radius of < 1 mm (near folding) mainly due to maximum local stretching in stress-concentrated regions. However, the resistance returned to the initial value with a minimal error of < 0.3 % when straightened. Although R_{norm} increased to 1.28 under twisting loads of up to 120 °, the initial electrical properties of the device were also recovered almost perfectly, as shown in Fig. 4d. Digital images in Fig. 4c and d show the devices under bending and twisting, respectively.

Fig. 5a shows a series of digital images of the LED circuit under stretching, bending, and twisting. The illumination intensity of the LED in each deformed state was almost constantly maintained without significant degradation compared to that in the undeformed state. When stretched to ~36 %, the LED circuit, which was operating at 3 V, was deactivated because of current reduction from the increased electrical resistance. However, the LED was immediately turned on upon releasing, and the initial illumination intensity

was recovered, as shown in Fig. 5b. This is attributed to the reversible behavior of the stretchable AgNW micro-grids under deformation, as suggested in Fig. 4. This clearly demonstrates that the stretchable AgNW micro-grids are greatly feasible for use as transparent conductors in emerging stretchable platforms owing to the superior electrical robustness (stretchability and reversibility) under various deformations.

Conclusions

In conclusion, AgNW percolation micro-grids were fully embedded in elastomeric substrate to demonstrate high-performance stretchable TCs. The TCs were prepared by a simple, low-cost, and potentially scalable fabrication method based on spray-coating and subsequent contact-removal of the AgNWs. The novel architecture combining a network structure of highly percolated AgNWs and a regular micro-grid geometry makes it possible to prepare high-performance stretchable TCs with uniform and reproducible performance. The fabricated device produced a low sheet resistance of 26.1 Ω/sq and high optical transmittance of 85.8 % (at 550 nm), which are comparable to the values of conventional ITO coatings. The device was found to be highly stretchable, bendable and twistable without permanent electrical or mechanical failure. The electrical properties of the device were also highly reversible for various mechanical deformations with minimal errors compared to the initial state. The stretchability and reversibility of the device were mainly attributed to reversible sliding of adjacent AgNWs in the percolated network during stretching and releasing. The electrical robustness against various mechanical deformations was experimentally confirmed through simple LED circuit demonstrations. The results suggest that the highly stretchable AgNW micro-grids can find many potential applications in emerging stretchable optoelectronics due to superior electrical conductivity and optical transmittance, and highly stretchable and reversible electrical behaviors.

Acknowledgements

This work was supported by a 2-Year Research Grant of Pusan National University.

Notes and references

[a] Department of Advanced Circuit Interconnection, Pusan National University, Busan 609-735, Republic of Korea.
[b] Department of Nano Fusion Technology and BK21 Plus Nano Convergence Technology Division, Pusan National University, Busan 609-735, Republic of Korea. *E-mail: jongkim@pusan.ac.kr
[c] Department of Cogno-Mechatronics Engineering, Pusan National University, Busan 609-735, Republic of Korea.

† Electronic Supplementary Information (ESI) available: SEM image, length and diameter distribution of the synthesized AgNWs (Fig. S1); optical transmittances of flat PDMS substrate in three different states; initial (bare), AgNW-coated, and contact-removed (Fig. S2); sheet resistances of AgNW micro-grids as a function of the number of coating-and-removal (C/R) cycle, and SEM images of the device processed with a single C/R process (Fig. S3); normalized electrical resistance under repetitive stretching/releasing (Fig. S4); transmittance spectra of the fabricated AgNW micro-grids with different grid-to-grid distance (Fig. S5); electrical resistances of the fabricated AgNW micro-grids in the loading states under tensile strains of up to 50 % and in the corresponding unloaded states (Fig. S6). See DOI: 10.1039/b000000x/

1. K. Ellmer, *Nat. Photonics*, 2012, **6**, 809.
2. R. B. H. Tahar, T. Ban, Y. Ohya and Y. Takahashi, *Journal of Applied Physics*, 1998, **83**, 2631.
3. T. Minami, *Semicond. Sci. Technol.*, 2005, **20**, S35.
4. S. Calnan and A. N. Tiwari, *Thin Solid Films*, 2010, **518**, 1839.
5. D. R. Cairns, R. P. Witte II, D. K. Sparacin, S. M. Sachsman, D. C. Paine, G. P. Crawford and R. R. Newton, *Appl. Phys. Lett.*, 2000, **76**, 1425.
6. J. Lewis, *Mater. Today*, 2006, **9**, 38.
7. T. Cheng, Y. -Z. Zhang, W. -Y. Lai, Y. Chen, W. -J. Zeng and W. Huang, *J. Mater. Chem. C*, 2014, **2**, 10369.
8. M. -S. Lee, K. Lee, S. -Y. Kim, H. Lee, J. Park, K. -H. Choi, H. -K. Kim, D. -G. Kim, D. -Y. Lee, S. Nam and J. -U. Park, *Nano Lett.*, 2013, **13**, 2814.
9. W. Hu, X. Niu, L. Li, S. Yun, Z. Yu and Q. Pei, *Nanotechnology*, 2012, **23**, 344002.
10. J. Liang, L. Li, K. Tong, Z. Ren, W. Hu, X. Niu, Y. Chen and Q. Pei, *ACS Nano*, 2014, **8**, 1590.
11. H. Lee, K. Lee, J. T. Park, W. C. Kim and H. Lee, *Adv. Funct. Mater.*, 2014, **24**, 3276.
12. W. Hu, R. Wang, Y. Lu and Q. Pei, *J. Mater. Chem. C*, 2014, **2**, 1298.
13. Y. Cheng, S. Wang, R. Wang, J. Sun and L. Gao, *J. Mater. Chem. C*, 2014, **2**, 5309.
14. D. J. Lipomi, M. Vosgueritchian, B. C-K. Tee, S. L. Hellstrom, J. A. Lee, C. H. Fox and Z. Bao, *Nat. Nanotechnol.*, 2011, **6**, 788.
15. X. Wang, T. Li, J. Adams and Jun Yang, *J. Mater. Chem. A*, 2013, **1**, 3580.
16. L. Cai, L. Song, P. Luan, Q. Zhang, N. Zhang, Q. Gao, D. Zhao, X. Zhang, M. Tu, F. Yang, W. Zhou, Q. Fan, J. Luo, W. Zhou, P. M. Ajayan and S. Xie, *Sci. Rep.*, 2013, **3**, 3048.
17. K. Liu, Y. Sun, P. Liu, X. Lin, S. Fan and K. Jiang, *Adv. Funct. Mater.*, 2011, **21**, 2721.
18. L. Xiao, Z. Chen, C. Feng, L. Liu, Z. -Q. Bai, Y. Wang, L. Qian, Y. Zhang, Q. Li, K. Jiang and S. Fan, *Nano Lett.*, 2008, **8**, 4539.
19. L. Cai, J. Li, P. Luan, H. Dong, D. Zhao, Q. Zhang, X. Zhang, M. Tu, Q. Zeng, W. Zhou and S. Xie, *Adv. Funct. Mater.*, 2012, **22**, 5238.
20. T. Chen, H. Peng, M. Durstock and L. Dai, *Sci. Rep.*, 2014, **4**, 3612.
21. Y. Zhang, C. J. Sheehan, J. Zhai, G. Zou, H. Luo, J. Xiong, Y. T. Zhu and Q. X. Jia, *Adv. Mater.*, 2010, **22**, 3027.
22. K. H. Kim, M. Vural and M. F. Islam, *Adv. Mater.*, 2011, **23**, 2865.
23. K. S. Kim, Y. Zhao, H. Jang, S. Y. Lee, J. M. Kim, K. S. Kim, J. -H. Ahn, P. Kim, J. -Y. Choi and B. H. Hong, *Nature*, 2009, **457**, 706.
24. M. Vosgueritchian, D. J. Lipomi and Z. Bao, *Adv. Funct. Mater.*, 2012, **22**, 421.
25. H. Y. Jang, S. -K. Lee, S. H. Cho, J. -H. Ahn and S. Park, *Chem. Mater.*, 2013, **25**, 3535.

26. C. F. Guo, T. Sun, Q. Liu, Z. Suo and Z. Ren, *Nat. Commun.*, 2014, **5**, 3121.
27. K. E. Korte, S. E. Skrabalak and Y. Xia, *J. Mater. Chem.*, 2008, **18**, 437.
28. A. D. Printz, E. Chan, C. Liong, R. S. Martinez and D. J. Lipomi, *PLoS One*, 2013, **8**, e83939.
29. P. -C. Hsu, S. Wang, H. Wu, V. K. Narasimhan, D. Kong, H. R. Lee and Y. Cui, *Nat. Commun.*, 2013, **4**, 2522.
30. Y. Zhu, Z. Sun, Z. Yan, Z. Jin and J. M. Tour, *ACS Nano*, 2011, **5**, 6472.
31. J. Wu, J. Zang, A. R. Rathmell, X. Zhao and B. J. Wiley, *Nano Lett.*, 2013, **13**, 2381.

Metal Nanowire Percolation Micro-Grids Embedded in Elastomer for Stretchable and Transparent Conductors

Sang-Min Park, Nam-Su Jang, Sung-Hun Ha, Kang Hyun Kim, Dong-Wook Jeong, Jeonghyo Kim, Jaebeom Lee, Soo Hyung Kim, and Jong-Man Kim*

Graphical Abstract

A new class of highly stretchable and transparent conductor based on silver nanowire (AgNW) percolation micro-grids prepared by spray-coating and subsequent adhesive-tape-assisted contact removal of AgNWs is presented.